Detailed Analysis of Differential Dynamics and Morphology in Polyisobutylene and Poly(isobutylene-*co*-*p*-methylstyrene) by Solid State NMR

Jeffery L. White,* A. J. Dias, and J. R. Ashbaugh

Exxon Chemical Polymer Science Division and Butyl Technology Division, 5200 Bayway Drive, Baytown, Texas 77522-5200

Received November 12, 1997; Revised Manuscript Received January 24, 1998

ABSTRACT: Polyisobutylene is unique among elastomeric polymers in that while the glass transition temperature is low (−70 °C), segmental dynamics at temperatures above T_g are relatively slow due to steric constraints resulting from the molecular packing of methyl groups. We describe results from NMR experiments on solid polyisobutylene (PIB) and copolymers with *p*-methylstyrene (PIB−PMS) in which the dynamics of chain motion in PIB homopolymers and PIB−PMS copolymers are compared as a function of temperature. Our one- and two-dimensional solid-state ^{1}H, ^{13}C, and ^{2}H results clarify previously published reports on local vs correlated segmental dynamics for the PIB homopolymer, which differ by 4−5 orders of magnitude in their correlation times. Distinct differences in aromatic ring dynamics as a function of PMS concentration are also observed for PIB−PMS copolymers. While PMS dynamics are found to be sensitive to PMS concentration in the copolymer, PIB motions appear to be independent of the comonomer incorporation. These results may be understood based on the clustered or blocky incorporation of PMS comonomer segments in the polymer chain. This copolymer system represents a regime intermediate between random copolymers and phase-separated block polymers and may be considered a correlated random copolymer. Relaxation and 2D HETCOR experiments are used to define morphology for the PMS clusters in the copolymer, and the results are consistent with a 3 nm domain size for the clusters. Finally, the effects of curing on dynamics at the cross-link site for functionalized PIB−PMS copolymers are selectively examined using ^{2}H wide-line experiments.

Introduction

Polyisobutylene is unique among synthetic polymers in that the WLF parameters which correspond to segmental motions increase at a much slower rate above the glass transition temperature relative to other elastomers with similar T_g values.[1−3] However, in many previous reports, the "segmental" dynamics of PIB are discussed in general terms. Bandis et al.[4] recently reported spin−lattice relaxation experiments on bulk PIB and concluded that the time scales for segmental motions in PIB were 10^{-9} s^{-1}. McGrath and co-workers concluded, based on the analysis of Rothwell−Waugh[5] effects, that the relevant time scale for segmental motion was ca. 10^{-4} s^{-1} over a similar temperature range.[6] Clearly, there needs to be an explanation of the large difference in time scales attributed to segmental motion in PIB and, more importantly, a clarification of the specific types of chain motion probed in the above NMR experiments. One problem that exists in previous literature is the general reference to "segmental motion" and its influence on experimental observables, while in fact there are several possible subsets of motional processes which are simultaneously operative. Such motions include the internal Rouse modes for chain-length fluctuations within the tube, chain diffusion within the tube, translation of the tube within the polymer matrix, and high-frequency monomeric librational or vibrational motions.[7]

We report the results from detailed variable-temperature rotating-frame relaxation and selective line-broadening (Rothwell−Waugh broadening[5]) experiments which unequivocally indicate the specific time scales for chain motions in bulk PIB. The correlation time for the motion responsible for line-broadening and $T_{1\rho H}$ relaxation is 1.4×10^{-5} s at 273 K. We assign this motion to correlated chain translation within the Rouse tube. Similar experiments for PIB−PMS copolymers, with varying PMS levels (2−28 mol %), reveal details about the dynamics of PMS aromatic rings as a function of PMS concentration, as well as the sensitivity of the same PIB segmental motions observed for bulk PIB to the PMS level. We were motivated to study solid-state dynamics for PIB−PMS copolymers, since Kennedy and co-workers have reported reactivity ratios and sequence distributions for PIB−PMS copolymers based on solution NMR data, and discovered that appreciable levels of PMS−PMS diads form at higher PMS comonomer concentrations.[8] Results indicating the formation of PMS clusters were confirmed in a similar study.[9] ^{1}H T_1 and $T_{1\rho}$ relaxation measurements along with solid-state 2D HETCOR/spin-diffusion experiments revealed the details about the microscopic morphology of these PMS clusters in the PIB−PMS copolymers. Functionalization of a small fraction of the PMS comonomer (via bromination) facilitates network formation via chemical cross-linking. Wide-line ^{2}H NMR and associated T_1 measurements were used to selectively probe the dynamics of the tie chain that forms as a result of curing.

Experimental Section

Number average molecular weights for the PIB polymers were 500K (polydispersity of 2.1), while the PIB-*co*-PMS materials were 100K. PIB−PMS copolymers were prepared at −100 °C by cationic polymerization in methylene chloride using isobutylene and *p*-methylstyrene as starting materials, with initiation promoted by ethylaluminum dichloride. Liquid nitrogen refrigerant was used for temperature control. Deu-

* Author to whom correspondence should be addressed. E-mail: jeffery.l.white@chemical.exxon.sprint.com. Tel: 281-834-5022. Fax: 281-834-2395.

S0024-9297(97)01670-7 CCC: $15.00
Published on Web 03/05/1998

terated samples were prepared in a similar manner using either PMS-d_4 or PIB-d_2 as starting materials.

Cross-linked samples were prepared by selective bromination of the PMS methyl carbon, resulting in a PIB−PMS−BrPMS terpolymer with a benzylic bromide group (1 mol % BrPMS) which could be displaced using a nucleophilic curative. Disodium hexamethlyene dithiosulfate was one such curative, and the perdeuterated (d_{12}) version was used for the wide-line dynamics experiments. These solid organic curatives were mixed into the polymer at 90 °C using a Banbury mill. Samples were cured at 160 °C for 10 min.

All NMR measurements were obtained on a Bruker DSX-500 intrument operating at a field strength equal to a ^{1}H Larmor frequency of 500.13 MHz. Pulse widths corresponded to $\pi/2$ flip angles and were typically 3−4 μs for ^{13}C or ^{1}H experiments. ^{2}H $\pi/2$ pulse widths were 2 μs, and the interpulse spacing in the solid-echo experiment was 20 μs. ^{1}H relaxation measurements were acquired indirectly via cross-polarization for T_1 and $T_{1\rho}$ experiments.[10] Cross-polarization contact times were 1 ms. 2D solid-state HETCOR (HETornuclear CORrelation) experiments employed an isotropic mixing sequence for polarization transfer[11] and were collected in a phase sensitive mode[12] using TOSS[13] for sideband suppression. 2D WISE data was collected as absolute value data, with the proton frequency offset from the carrier frequency, and a 500 μs contact time.[14]

Results and Discussion

The chemical structures for the PIB−PMS and PIB−BrPMS copolymers are

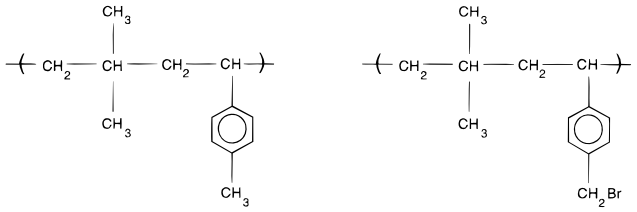

As mentioned above, previous work by Kennedy has shown that as the PMS concentration in the polymer increases from 2.4 to 8.6 mol %, the number of randomly incorporated (isolated) PMS units decreases from 52% to 23%. This corresponds to an increase in PMS sequence number from 3 to 11 as the [PMS] increases from 5 to 29 mol % in the polymer (where the sequence number is defined as the average number of uninterrupted sequences of like monomer units per 100 monomer units in the copolymer). However, before the effects of [PMS] on the copolymer dynamics may be assessed, chain dynamics in the PIB homopolymer must first be established.

Cross-polarization magic-angle spinning spectra of polyisobutylene homopolymer are shown in Figure 1 as a function of temperature. Since we are interested in segmental dynamics for the PIB, examination of the methylene resonance at 60 ppm is most informative. At high temperatures, a single sharp peak is observed, while conformationally inequivalent signals are observed near T_g (−60 °C). However, as the temperature increases from T_g, these signals become broad, and in fact, a complete loss of the methylene resonance is observed at 0 °C. These results are similar to those recently reported by McGrath et al., except the methylene resonance in their spectra is completely broadened at all temperatures at or below 0 °C.[6] This led the authors to conclude that the chain dynamics in PIB changed little over the −133 to 0 °C temperature range. This conclusion does not agree with our data in Figure

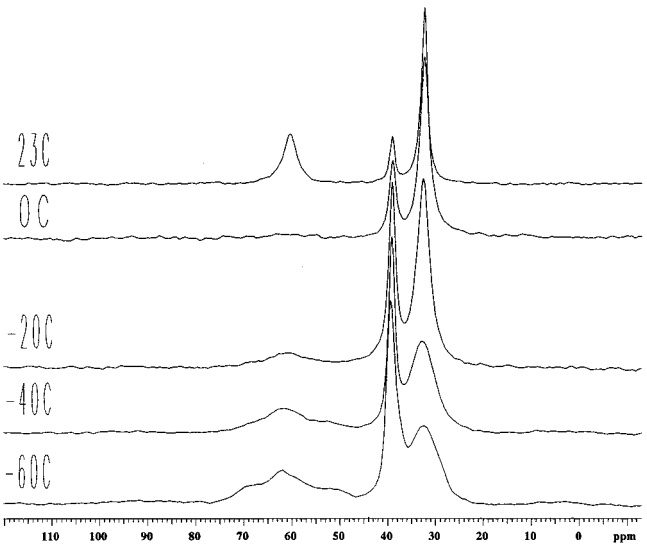

Figure 1. Variable-temperature cross-polarization magic-angle spinning spectra of polyisobutylene showing the temperature dependence of the methylene group line width at 60 ppm. The ^{1}H decoupling field strength was 71 kHz, and the spinning rate was 4.5 kHz. Note that a well-defined temperature is observed for the maximum line width at 0 °C.

1; we observe resolved trans−trans, trans−gauche, and gauche−gauche conformations at low temperatures, and a well-defined maximum line width at 0 °C. Experiments in which the ^{1}H decoupling rf field strength was varied revealed that as γB_{1H} was increased from 66 to 125 kHz, the methylene line width in the 23 °C spectrum decreased from 320 to 250 Hz. Intermediate rf powers produced line widths between these two limits at room temperature. Therefore, we conclude that the mechanism of line broadening for the methylene resonance at 60 ppm in Figure 1 is the so-called Rothwell−Waugh effect.[5] It is well-known that whenever an incoherent or stochastic molecular motion occurs on the same time scale as an experimentally introduced coherent averaging mechanism (in this case heteronuclear decoupling), the efficiency of the coherent averaging is reduced. There must exist some chain fluctuations in PIB with a maximum in the distribution of correlation times equal to $(71 \times 10^3\ s^{-1})^{-1}$ at 0 °C.

We may further investigate the time scale for chain dynamics in PIB using variable-temperature $T_{1\rho H}$ experiments. Shown in Figure 2 is a graph of the relaxation time constants for the methylene protons of PIB as a function of temperature. Again, a well-defined minimum is observed at 0 °C, consistent with the Rothwell−Waugh broadening. One would expect a minimum in the relaxation curve to appear at the same temperature as observed for the maximum line width in the CP spectra, since the same ^{1}H rf field strengths were used for decoupling and spin-locking. We would conclude, on the basis of these data, that the correlation time for segmental dynamics in the PIB homopolymer is 1.4×10^{-5} s at 0 °C.

While the above experiments and data analyses are straightforward, the results would seem to disagree with recent reports by Bandis et al. in which they reported segmental correlation times for PIB of 10^{-9}−10^{-10} s over a similar temperature range.[4] These correlation times are 4−5 orders of magnitude removed from what we observe in the high-resolution experiments above and were derived from variable-temperature T_{1C} measurements. Bandis and co-workers refer to the type of

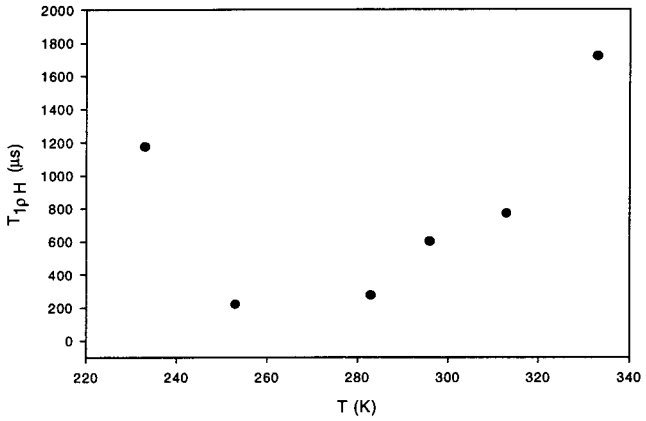

Figure 2. Relaxation plot for the ^{1}H $T_{1\rho}$ as a function of temperature. Note that the minimum relaxation time appears to occur near 273 K (0 °C), the same temperature observed for the maximum line width of the methylene signal in Figure 1. Here, $\gamma B_{1H} = 71$ kHz.

segmental motion probed in their experiments as arising from conformational changes in the polymer backbone. Clearly, a clarification for the discrepancy in time scales for motions assigned as "segmental" motions is required, as we must also be probing changes in backbone conformation since the conformationally inequivalent methylene signals observed at −60 °C become exchange averaged as the temperature is increased. (In fact, the exchanged averaged methylene line shape sets a lower limit on the frequency of backbone reorientation, since the 20 ppm spread in chemical shift dispersion is eliminated. The corresponding frequency for motion, therefore, exceeds 2.5 kHz.) High-frequency motions of the type probed by a T_1 or NOE experiment may correspond to either librational motions or uncorrelated conformational rearrangements of monomeric scale units, i.e., lower Rouse modes. Motions characterized by frequencies in the kilohertz regime for PIB must correspond to correlated, reorientational diffusion of the chain within the Rouse tube. Our interpretation of these data is consistent with early NMR experiments by Komoroski and Mandelkern, in which they observed no dependence of T_1 and NOE on the PIB molecular weight.[15] Such a result would be expected for high-frequency motions whose distribution is not correlated with other chain segments. However, in proton-decoupled ^{13}C spectra, obtained without MAS, those authors observed a significant difference in the temperature at which a motionally narrowed "high" resolution spectra was measured for different molecular weights. Again, this is consistent with reorientational diffusion of the chain, where individual chain segments change the directions of their bond vectors in a cooperative manner relative to other segments in the chain. Of course, there exists a distribution in correlation times for the collective modes being probed by Rothwell−Waugh and $T_{1\rho}$ measurements.

Given knowledge of the PIB behavior outlined above, one may now approach dynamics in the PIB−PMS copolymers. Variable-temperature CP spectra are shown for two PIB−PMS (2.5 vs 13.8 mol % PMS) copolymers in Figure 3. The first thing to note is that the temperature at which the maximum line width is observed for the PIB methylene carbons at 60 ppm is still 0 °C, just as in the homopolymer. Examination of the aromatic carbon resonance at 128 ppm and its associated spinning sidebands indicates a similar Rothwell−Waugh

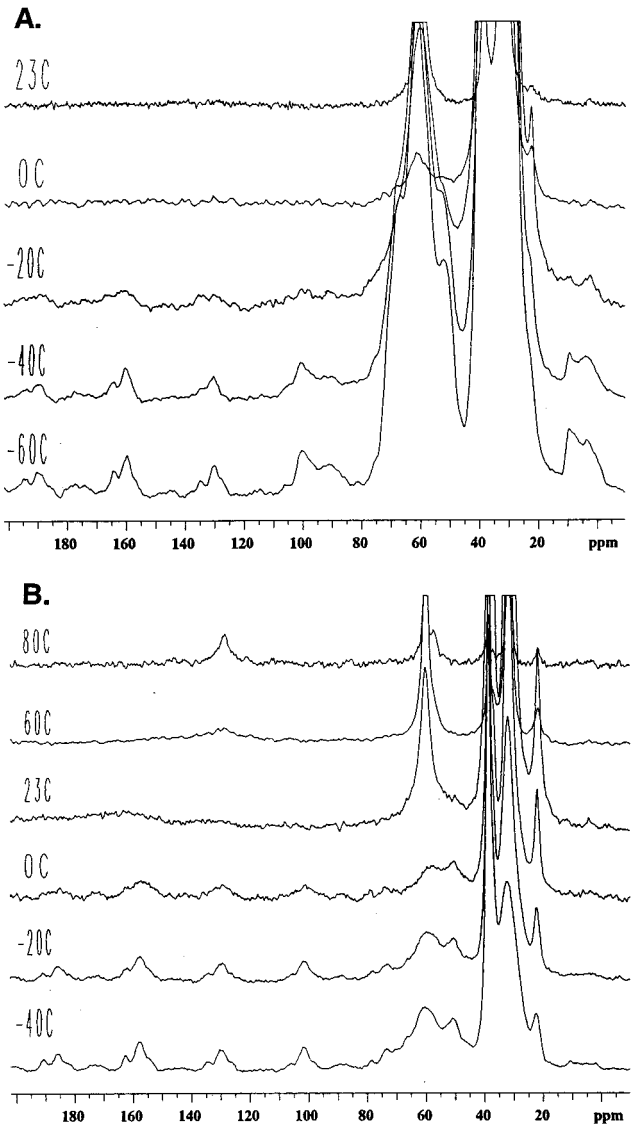

Figure 3. Stack plots of the CP/MAS spectra for (a) PIB/PMS (2.5 mol %) and (b) PIB/PMS (13.8 mol %) copolymers as a function of temperature, demonstrating the difference in temperatures at which the maximum Rothwell−Waugh broadening is observed for the PMS aromatic signals as a function of mol % of PMS in the copolymer. The PMS aromatic signals do not cross-polarize above room temperature for the 2.5 mol % sample.

Table 1. Temperature Dependence of Rothwell−Waugh Line Broadening for the PMS Aromatic Signal in PIB-*co*-PMS

mol % PMS	temp of max line width (K)	mol % PMS	temp of max line width (K)
2.4	273 K	14	318 K
4.3	273 K	28	373 K
7	296 K		

linebroadening behavior as was observed for the PIB. However, the temperatures at which the aromatic resonance reaches maximum breadth is clearly different for the 2.5 vs 13.8 mol % PMS samples. Table 1 lists the temperature of maximum line width for the PMS aromatic signal at 128 ppm as a function of mol % of PMS (2.4−28%) in the polymer. The temperature of maximum line width corresponds to the temperature at which the phenyl rings in the PMS units undergo reorientational motion (presumably ring flips about the backbone-ring C−C bond) on a time scale equal to the

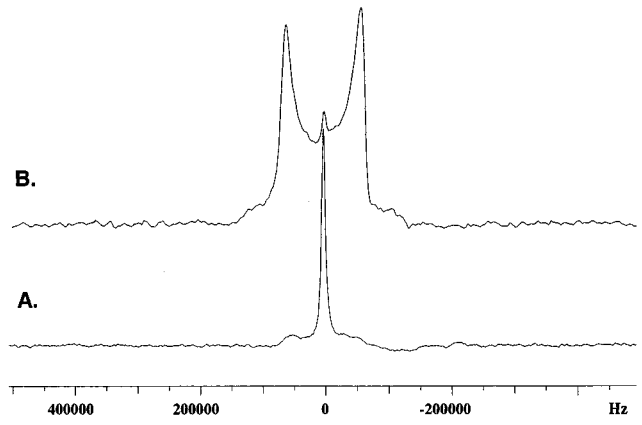

Figure 4. Wide-line ^{2}H NMR spectra for (a) PIB/PMS-d_4 (3 mol %) and (b) PIB/PMS-d_4 (25 mol %). Note the small fraction of mobile aromatic rings in b.

inverse of the ^{1}H decoupling field strength. Given our knowledge of the increasing PMS−PMS sequence numbers at higher PMS levels from Kennedy's work and on the basis of the observed composition dependence of the PMS aromatic signal from Rothwell−Waugh broadening, we believe that the dynamics of the rings become controlled by cooperative ring flips as more PMS is incorporated in the copolymer. At higher PMS concentrations, the probability that PMS monomer units are incorporated between neighboring PMS groups, or clusters, increases and the dynamics become governed by the correlated ring motions known to exist in polystyrene. At low concentrations of PMS in the polymer, the temperature for maximum broadening of the 128 ppm signal is 0 °C, the same as that for the methylene carbons of the PIB backbone. This suggests that, at low PMS concentrations, ring dynamics of the PMS monomer units are controlled by PIB reorientational fluctuations characteristic of that homopolymer.

We support these conclusions based on ^{2}H wide-line experiments. Static ^{2}H spectra are shown in parts a and b of Figure 4 for a PIB−PMS copolymer containing 3 mol % and 25 mol % PMS-d_4, respectively. For the 3 mol % PMS sample, the majority of aromatic rings have sufficient mobility to completely average the quadrupolar coupling, and a narrow peak of width 10 kHz is observed. A rigid quadrupolar Pake pattern with a central splitting of 120 kHz is measured for the 25 mol % PMS sample, similar to that reported for polystyrene-d_5.[16] Only a small fraction of mobile PMS deuterons are observed as the narrow central peak. Further evidence that the incorporation of PMS in the copolymer is blocky comes from the observation of a small fraction of rigid aromatic rings in Figure 4a for the 3 mol % PMS. One may assign the narrow component in parts a and b of Figure 4 to randomly incorporated PMS monomer units, since the line width of 10 kHz is reduced from that measured for deuterated methylene carbons in PIB-d_2/PMS copolymers. A similar experiment on a 2.8 mol % PMS/PIB-d_2 polymer showed a motionally narrowed spectrum with a 30 kHz line width for the methylene deuterons (spectrum in Figure 4c). A consistent picture emerges; at low PMS levels, aromatic rings which are isolated or at very short run lengths between PIB units in the chain are motionally averaged at room-temperature both by the PIB backbone reorientation discussed earlier and by fast rotation about the PMS backbone−ring C−C bond. These two motions together act to reduce the PMS deuterium line width below that

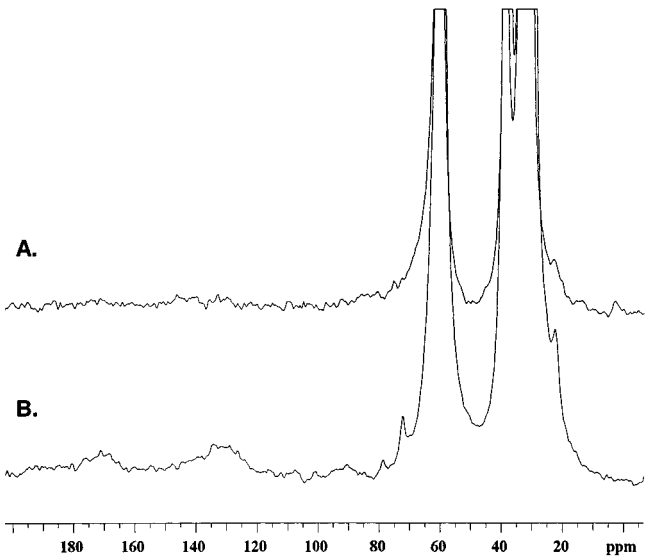

Figure 5. Room-temperature CP/MAS spectra for an (a) uncured and (b) cured PIB/PMS (2.5 mol %) copolymer. The PMS aromatic ring signals at 130 ppm become visible at this temperature after curing, since the frequency of ring dynamics is shifted by chemical cross-linking.

observed for the PIB backbone, which is consistent with our observation in Figure 3a that the aromatic PMS signals do not cross-polarize at room temperature for the 2.5 mol % sample but the PIB methylene signals do. At PMS levels of 25% in the polymer, the majority of PMS monomer units exist in clusters or blocks of repeat PMS monomers, and aromatic ring flips must occur in concert with neighboring rings.

For the low PMS copolymers, introduction of chemical cross-linking perturbs the reorientational dynamics of the isolated rings. Shown in Figure 5 are the room-temperature CP spectra for PIB−PMS (2.5 mol %) copolymers, before and after cross-linking. The protonated aromatic carbon signals at 130 ppm and its spinning sidebands become visible following cross-linking, indicative of an increase in the correlation time for aromatic ring motion.

The temperature-dependent Rothwell−Waugh maxima and ^{2}H data described above show that the dynamics of PMS monomer units are dependent on PMS concentration in the polymer. We are also interested in determining how the molecular dynamics of the PIB monomer units in the copolymer are affected by the change in PMS concentration. As the PMS level increases in the copolymer, one might expect that the time scale for reorientation of the entire polymer chain decreases in a homogeneous fashion for any monomer or segments of monomers in the chain, as was observed above for the PMS units. The first seven slices from a room temperature 2D WISE experiment[14] on PIB/PMS (28 mol %) are shown in Figure 6. This particular sample was chosen since it contains a high PMS level, and the experiments described above showed that the PMS units exist in a highly constrained, rigid environment. In the 2D WISE experiments, signals from rigid portions of the polymer will decay quickly, while signals from mobile polymer segments will persist for longer times. The basis of this discrimination is the attenuation of homonuclear dipolar couplings between protons by molecular motion. As is easily seen in the figure, both the aromatic and aliphatic signals from the PMS decay after only 15 μs, while the PIB signals persist past

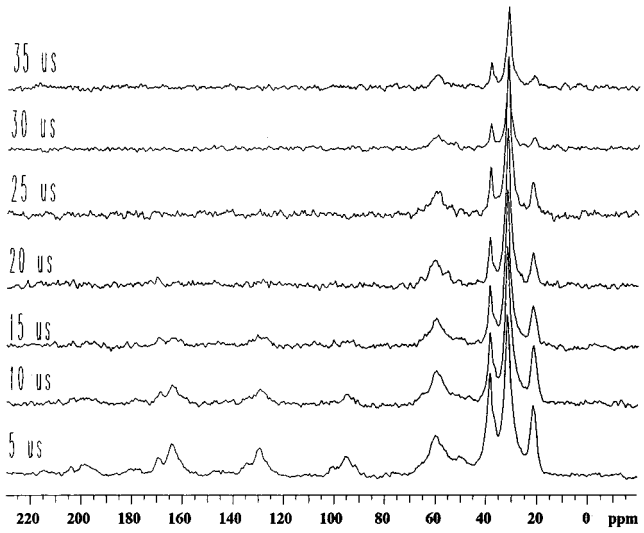

Figure 6. Plot of the first seven slices from a 2D WISE experiment on PIB/PMS (28 mol %) copolymer. The effective T_2 for the PMS signal is 10 μs compared to 32 μs for the PIB methylene signal.

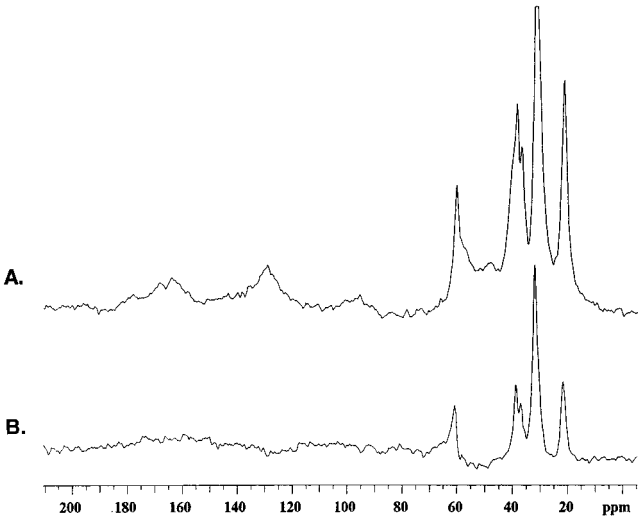

Figure 7. CP/MAS spectra obtained at 80 °C for the sample in Figure 7 without (a) and with (b) 60 μs of interrupted proton decoupling.

100 μs. Plots of the signal intensity vs dephasing time from the WISE data give an effective T_2* for PIB segments of 31 vs 10 μs for PMS units. One should note that the WISE sequence used here did not have a ^{1}H spin−echo prior to CP but only a 90° pulse. Therefore, one would expect a shorter decay constant for the PIB relative to the 55 μs value we measured with a standard CPMG sequence for a PIB homopolymer.

One final experiment was performed to demonstrate that even though the PIB/PMS (28 mol %) sample is a copolymer, segmental dynamics of the PIB units are essentially independent of the PMS dynamics. Shown in Figure 7 is the CP spectrum of the same polymer as in Figure 6, obtained without (Figure 7a) and with (Figure 7b) 60 μs of interrupted proton decoupling.[17] The spectra were obtained at 80 °C, a temperature intermediate between the points of maximum line-broadening for either the PIB methylene signal or the PMS aromatic signal. This temperature was also chosen since resolved signals for the PIB quaternary carbon are observed, corresponding to polyisobutylene quaternary carbons in PIB−PIB vs PIB−PMS diads (37−40 ppm).

Table 2. ^{1}H Spin−Lattice Relaxation Parameters for PIB and PMS Homopolymers and the PIB−PMS (28 Mol %) Copolymer

	$T_{1\rho}$ (^{1}H) (ms)	T_1 (^{1}H) (ms)
	Homopolymers	
PIB CH_2	0.6	375
PIB CH	1	427
PMS CH/CH_2	11.5	1.34×10^3
PMS ring CH	11	1.4×10^3
	Copolymer	
PIB CH_2	3	505
PIB CH	3.2	515
PMS ring CH	5.8	600
PMS CH/CH_2	5.7	575

The PMS signals are completely dephased after the period of interrupted decoupling, while the PIB signals remain. We also note that both PIB quaternary carbon signals for the PIB−PIB diads vs PIB−PMS diads survive as well. Together, these data indicate that the dynamics of PIB units in the copolymer chain are independent of PMS dynamics, even at the higher PMS levels which cause a shift in time scales for PMS dynamics. The apparent independence of comonomer segmental dynamics in a copolymer which is not phase separated is surprising, but conceptually analagous to the unique dynamics observed for different polymer chains in blends which are miscible at the molecular level.[18,19]

TEM micrographs were obtained on three copolymer samples containing different PMS concentrations in the polymer (6.5, 14, and 28 mol %). Phase structure which could be assigned to distinct domains was not visible for any of the samples at the 20 nm level or greater. To further address the maximum size of any domains formed in these high [PMS] copolymers, relaxation measurements were done on the PIB−PMS (28 mol %) sample. The relaxation data for T_{1H} and $T_{1\rho H}$ measurements at 23 °C on PIB and PMS homopolymers as well as the PIB−PMS copolymer are shown in Table 2. The interpretation of relaxation data with respect to length scales is by now well understood, based on several experiments primarily aimed at probing molecular miscibility in polymer blends.[20] In short, spin diffusion among protons is operative in both the T_{1H} and $T_{1\rho H}$ experiments (although scaled by a factor of 0.5 in the $T_{1\rho H}$ experiment), and given the length of the relaxation time constant, one can determine upper and lower limits for characteristic domain sizes. The data in Table 2 show that for the T_{1H} experiment, the measured value for the PIB−PMS (28 mol %) copolymer is intermediate compared to either homopolymer, and the same value (within the error of the data analysis) is obtained for measurement of either PMS or PIB signals of the copolymer. Analysis by the standard equation for approximating the length scale x of spin diffusion[21]

$$x = \sqrt{\frac{4}{\pi} \mathrm{D}t}$$

where x is the distance over which spin diffusion propagates during a time $t = T_1$, gives an upper length scale of PMS clusters of 23 nm. D is the spin diffusion constant, which was recently reported to be 8×10^{-12} cm^2/s by Spiess and co-workers.[22] However, the $T_{1\rho H}$ data in Table 2 shows that while the relaxation times for the PIB and PMS hydrogens in the copolymer are changed significantly toward intermediate values rela-

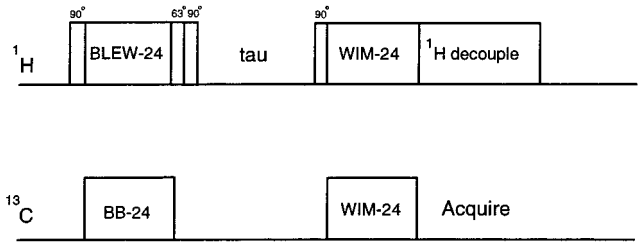

Figure 8. Pulse sequence used for the 2D HETCOR measurements. Spin diffusion occurs during the τ period, which was omitted for the normal HETCOR experiment. The BB-24, BLEW-12, and WIM-24 blocks are composed of phase alternated $\pi/2$ pulses on each channel. One WIM cycle was used for polarization transfer.

tive to the homopolymers, they do not converge to the same value. If one takes the 3 ms $T_{1\rho H}$ measured for the PIB signals, analysis by the same diffusion equation above yields a length scale of 1.8 nm. Since the PMS signal $T_{1\rho H}$ is approximately twice as long as the PIB, then the individual monomer units of the clusters of PMS segments are not, on average, mixed homogeneously with the PIB monomer units on a 1.8 nm length scale. Therefore, the characteristic size of the PMS clusters in the PIB/PMS (28%) copolymer is between ca. 1.8 and 23 nm based on the relaxation data.

Two-dimensional solid-state HETCOR techniques were used to more accurately determine the characteristic size of the clustered PMS domains in this copolymer. The HETCOR technique is particularly useful for the study of polymers, since the poor resolution associated with the CRAMPS approach is enhanced due to the dispersion by the carbon chemical shift. Recent investigations of polymer systems by this technique have been successful in elucidating phase structure[23] and chemical interactions[24] in polymer blends. We have used the spin-diffusion variant of the HETCOR sequence in a manner similar to that recently reported by Kaplan for the study of polycarbonate blends.[25] The pulse sequence is shown in Figure 8, where the homonuclear proton dipolar mixing occurs during the delay between the BLEW-24 evolution time and the WIM polarization transfer period. For the standard HETCOR sequence without spin-diffusion, this delay was omitted.

Figure 9a shows the results from the HETCOR experiment without spin-diffusion for the same PIB−PMS (28 mol %) copolymer used in the relaxation experiments. Correlations are observed connecting the carbon spectrum with their directly attached hydrogens in the proton dimension. We observe that the PIB methyl (^{13}C δ = 30 ppm) and PMS methyl (^{13}C δ = 20 ppm) hydrogens have distinctly different chemical shifts, consistent with solution NMR values. Also, note that for this experiment where there is no spin diffusion time, the aliphatic carbons show no correlation to aromatic hydrogens and vice versa.

Spin-diffusion, and therefore any microscopic morphology, may be monitored by observing aliphatic-to-aromatic correlations as a function of the mixing time. Shown in Figure 9b−d are the HETCOR plots for mixing times of 100 μs, 500 μs, and 5 ms, respectively. We specifically focus on the growth of the aliphatic proton correlations for the aromatic carbons at 130 ppm and the aromatic proton correlations for the PIB methyl carbon and the PMS methyl carbon. A graphical representation of the ratios of the aliphatic:aromatic ^1H intensity, obtained by taking slices through the carbon chemical shifts for the PIB methyl and PMS methyl and aromatic carbons, as a function of the spin diffusion time is shown in Figure 10. At thermal equilibrium for the proton dipolar spin reservoir, spin diffusion will render all proton slices through any carbon signal equivalent. These particular signals were chosen since they are completely resolved, and the PMS aromatic and methyl carbons allow us to probe spin-diffusion within the PMS monomer, while the PIB methyl signal provides a potential probe of spin diffusion between the PMS clusters and neighboring intrachain and interchain PIB segments.

Figure 10 shows that the PMS signals converge to the same ratio quickly, on the order of 500 μs. However, the time required for the PMS and PIB signals to reach the common, equilibrium ratio is much longer at 5−10 ms. We also note that the PMS methyl and PIB methyl protons also converge to the same chemical shift. The rapid convergence of the PMS signals is consistent with the presence of aromatic and aliphatic hydrogens within that monomer unit. The order of magnitude difference observed for the PMS−PMS correlations relative to the PMS−PIB correlations would not be expected if the PMS was randomly incorporated as isolated monomer units in the PIB backbone. Using the times required to reach equilibrium from Figure 10 (5−10 ms), we estimate that the characteristic size of the PMS clusters in the PIB/PMS (28 mol %) sample to be 3 nm. These results are similar to recent reports of PS clusters formed in miscible PPO/PS-d_5 blends.[23]

Our length scale calculations based on the 2D solid-state HETCOR results are in agreement with control experiments on the same polymer obtained using small-angle neutron scattering. Details from this study will be reported at a later time.

Recall the data in Figure 5 which showed that the time scale for aromatic ring reorientation in PMS is reduced upon introduction of chemical cross-linking, even for a copolymer having only 2.5 mol % total PMS and 1 mol % BrPMS. These results motivated us to specifically consider the molecular dynamics of a tie-chain which forms at the cross-link site after curing the PIB−PMS−BrPMS terpolymer. A perdeuterated disodium hexamethlyenedithiosulfate curative (d_{12}) was introduced, and static ^2H wide-line NMR spectra were obtained as a function of curative for uncured and cured materials (see Figure 11). Presumably, reaction of the bifunctional curative with two neighboring BrPMS sites proceeds as shown in the following scheme:

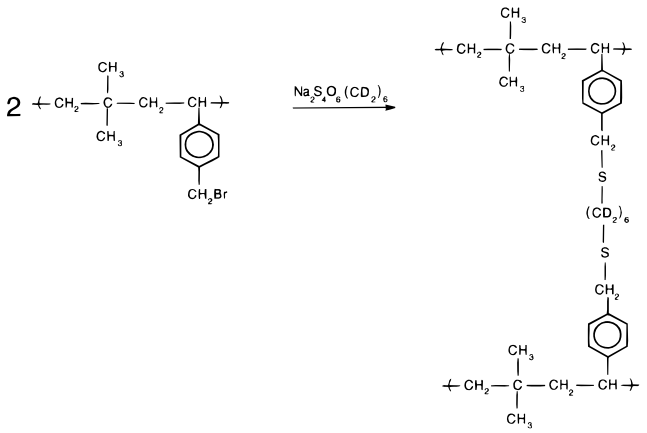

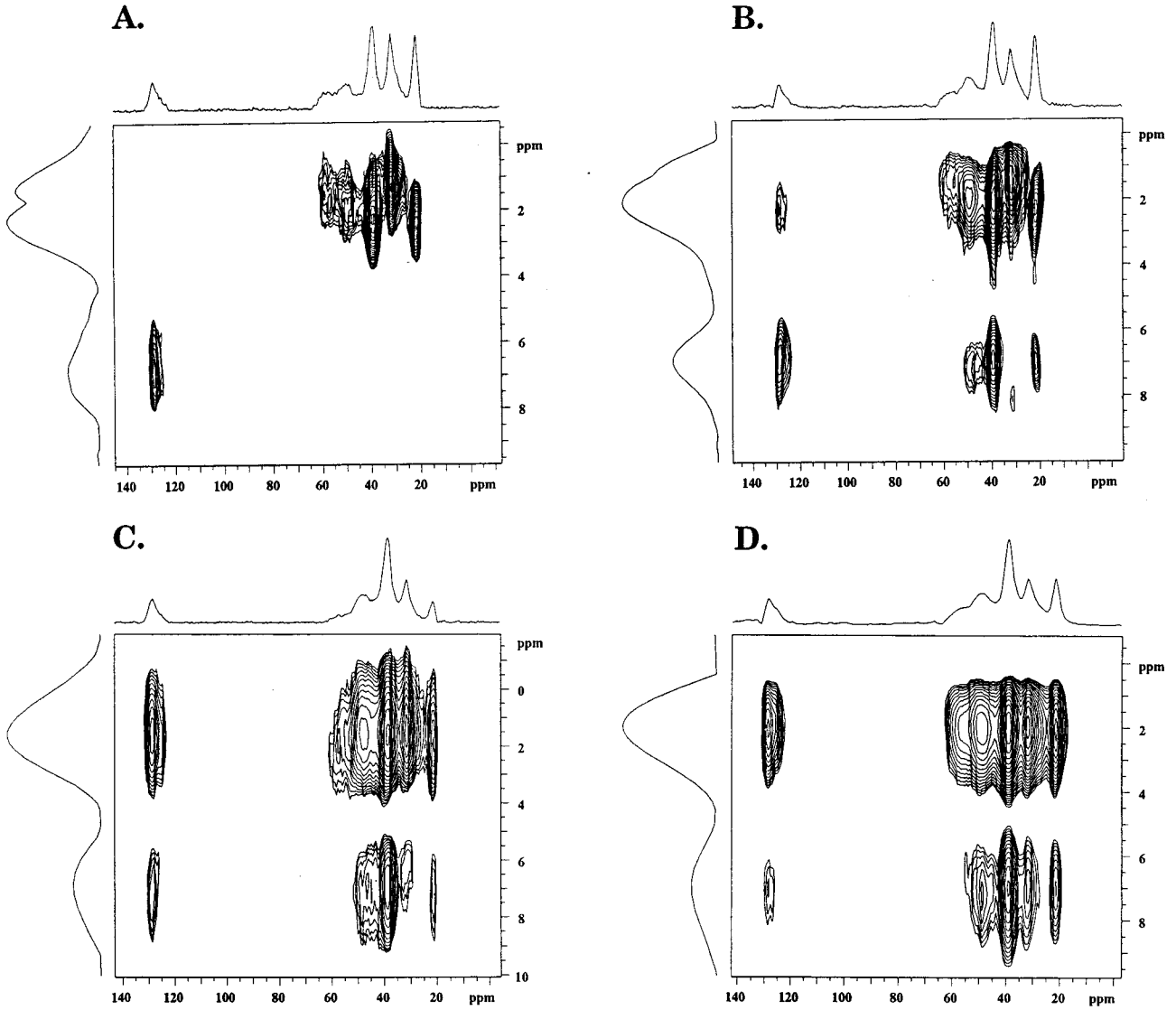

Figure 9. 2D HETCOR/TOSS spectra for the PIB/PMS (28 mol %) obtained using the sequence in Figure 8 with (a) 0, (b) 100 μs, (c) 500 μs, and (d) 5 ms spin-diffusion times. Note in particular the time-dependence of the ^{1}H aliphatic correlation at the aromatic ^{13}C chemical shift (128 ppm) and the aromatic correlations at the methyl ^{13}C shifts (21 and 31 ppm).

Figure 11a shows the spectrum for the neat curative, which is a crystalline solid. The measured splitting of the horns in Pake powder pattern is 113 kHz, which corresponds to a quadrupolar coupling constant equal to 150 kHz. Parts b−g of Figure 11 are the spectra for three different curative loadings, before and after curing. The three loadings correspond to increasing curative:cure site ratios. Spectra b and c from Figure 11 correspond to 1 equiv of curative per 4 equiv of BrPMS cure sites, while the curative:BrPMS ratios for Figure 11d,e and Figure 11f,g are 1:1 and >2:1, respectively. Several features of these data require clarification. First, we notice that, with the exception of spectrum f from Figure 11, comparisons of the cured and uncured spectra look very similar for each loading; i.e., a rigid component of equal intensity remains after curing. Comparison of the uncured sample spectra (Figure 11b,d,f) suggest that the broad component in the uncured samples is neat curative which has not reacted, since the signal intensities in these spectra increase in a manner consistent with the increased curative loadings. ^{2}H T_1 measurements confirmed this; the T_1 for the neat curative (Figure 11a), measured at the horn, was 1 s. The T_1 for the rigid fraction in the uncured samples was also 1 s. Upon curing, the T_1 for the rigid component is reduced to 30 ms. Second, the relative fraction of the narrow central component increases after curing for the 1:1 and >2:1 samples in Figure 11d−g, but remains constant in Figure 11b,c. The experimentally measured T_1 for the narrow component in these spectra was 20 ms for Figure 11d−f, and 10 ms for the spectrum in Figure 11g. Figure 11g is particularly striking, in that the majority of the ^{2}H signal comes from methylene groups in a motionally narrowed environment.

Our intepretation of the differences in the relative fraction of the narrow vs broad components in Figure 11 is based on the fact that the disodium hexamethylenedithiosulfate is a bifunctional curative. As such, each curative molecule may react with either one or two BrPMS groups. In the 1:4 curative:BrPMS sample, in which there was an excess of reactive sites on the polymer, the majority of the curative reacts in the desired bifunctional manner and forms a cross-link site between PMS groups on neighboring chains. The six carbon bridging chain does not undergo any large-amplitude motions on a time scale short enough to narrow the Pake pattern, yet the reduced T_1 value of

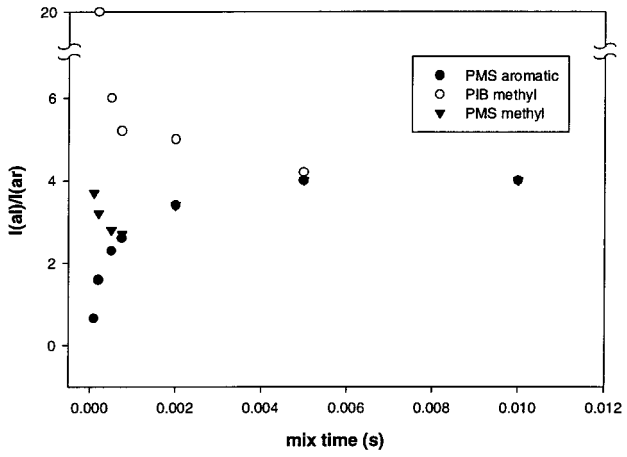

Figure 10. Plots of the ^{1}H aliphatic:aromatic intensities through the slices of the respective cross-peaks for the PMS aromatic carbon (128 ppm), PMS methyl carbon (21 ppm), and the PIB methyl carbon (31 ppm). Note the rapid convergence of the PMS signals to a common ratio, followed by the long time equilibration with the PIB methyl signal. See text for detailed explanation.

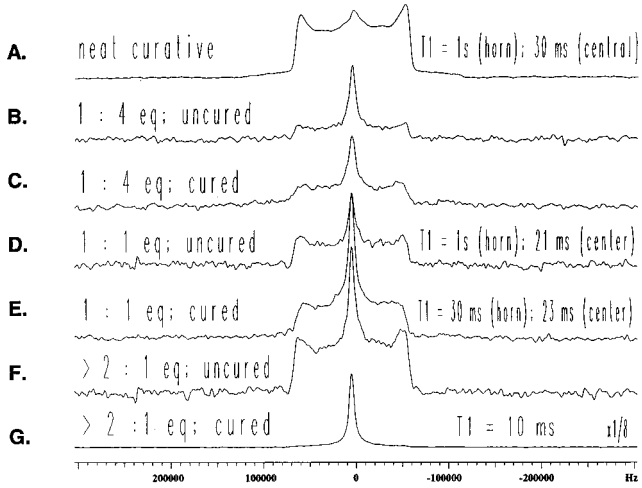

Figure 11. Wide-line ^{2}H NMR data for the perdeuterated disodium hexamethylenedithiosulfate curative neat (a), and in varying concentrations relative to the BrPMS level in the PIB−PMS−BrPMS terpolymer, either cured or uncured (b−g). The curative:cure site ratios are as follows: (b) 1:4 uncured; (c) 1:4 cured; (d) 1:1 uncured; (e) 1:1 cured; (f) >2:1 uncured; (g) >2:1 cured. Data for part g are is scaled by a factor of $^1/_8$.

30 ms relative to 1 s for the neat curative indicates the presence of high-frequency librational motions. The 1:1 and >2:1 samples in Figure 11d and Figure 11g clearly undergo more monofunctional reactions, and possibly curative−curative reactions, since the fraction of the narrow component increases after curing. The increase in the narrow component is most striking for the sample in Figure 11g which has a large excess of curative and is therefore most prone to undergo reactions which do not lead to the formation of a network.

The network density, or degree of cross-linking, must be the greatest in the sample with the lowest curative: cure site ratio Figure 11c. This is indeed the case, as shown by the plot in Figure 12 in which the relative fraction of the broad component arising from the tie chain in the cured samples is plotted against the swelling ratio. Clearly, the incorporation of the deuterated curative into the motionally constrained sites corresponds to an increased network density, and the probability for that incorporation is reduced as the curative loading is increased.

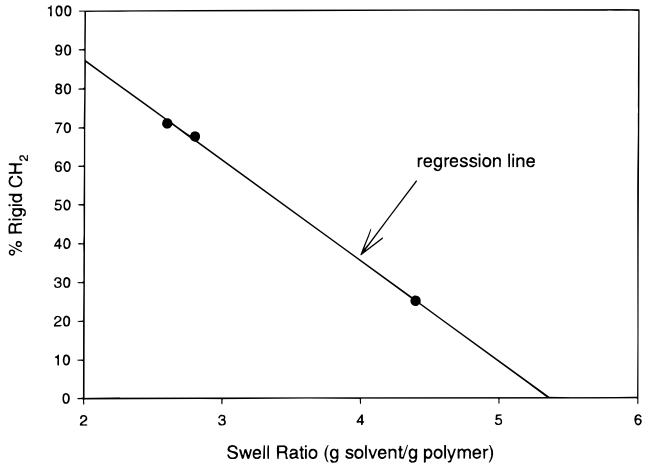

Figure 12. Plot of the fraction of rigid Pake pattern of the disodium hexamethylene dithiosulfate curative from the three cured samples in Figure 11c,e,g vs the swell ratio in toluene.

Conclusions

We have demonstrated that solid-state NMR provides unique information concerning specific molecular and chain dynamics in the polyisobutylene homopolymer and its copolymer with *p*-methylstyrene. Relaxation analysis and spin-diffusion experiments revealed that the length scale of the PMS clusters or blocks that form at high PMS concentrations in the copolymer to be 3 nm. The PIB−PMS copolymer is heterogeneous both with respect to chain dynamics and morphology, which increases as the PMS concentration increases in the copolymer. While the PMS clusters exhibit dynamics similar to polystyrene at high PMS concentrations (e.g. 25 mol %), the PIB dynamics appear to be independent of the PMS loading. We believe that such heterogeneity may cause difficulties in functionalization or cure chemistries of copolymers with high PMS levels.

Microphase separation in correlated random copolymers, which includes the PIB−PMS copolymers described here, has been anticipated by a number of theoretical papers.[26−28] The papers determine that both the segmental interaction parameters and the sequence run length play an important role in determining microphase separation. In addition, these systems are predicted to have limited long-range order, as we have described above from the NMR data, and unusual temperature sensitivity at the order−disorder transition. We believe that such heterogeneity may cause difficulties in functionalization or cure chemistries of copolymers with high PMS levels. Our future efforts will be directed toward understanding the different chemistries that we believe will occur as a function of correlated comonomer clusters in these systems.

References and Notes

(1) Boyd, R. H.; Pant, P. V. K. *Macromolecules* **1991**, *24*, 6325.
(2) Dekmezian, A.; Axelson, D. E.; Dechter, J. J.; Borah, B.; Mandelkern, L. *J. Polym. Sci., Polym. Phys. Ed.* **1985**, 23, 367.
(3) Boyd, R. H.; Pant, P. V. K. *Macromolecules* **1992**, *25*, 494.
(4) Bandis, A.; Wen, W.; Jones, E. B.; Kaskan, P.; Zhu, Y.; Jones, A. A.; Inglefield, P. T.; Bendler, J. T. *J. Polym. Sci. B, Polym. Phys.* **1994**, *32*, 1707.
(5) Rothwell, W. P.; Waugh, J. S. *J. Chem. Phys.* **1981**, *74*, 2721.

(6) McGrath, K. J.; Ngai, K. L.; Roland, C. M. *Macromolecules* **1992**, *25*, 4911.
(7) Graessley, W. W. *Physical Properties of Polymers*, 2nd ed.; American Chemical Society: Washington, DC, 1993; p 130.
(8) Lubnin, A.; Orszagh, I.; Kennedy, J. P. *J. M. S. Pure Appl. Chem.* **1995**, *A32*, 1809.
(9) Cheng, D. M.; Wang, H. C. Unpublished results.
(10) Sullivan, M. J.; Maciel, G. E. *Anal. Chem.* **1982**, *54*, 1615.
(11) Caravatti, P.; Bodenhausen, G.; Ernst, R. R. *Chem. Phys. Lett.* **1982**, *89*, 363.
(12) Burum, D. P.; Bielecki, A. *J. Magn. Reson.* **1991**, *94*, 645.
(13) Dixon, W. T.; Schaefer, J.; Sefcik, M.; Stejskal, E. O.; McKay, R. A. *J. Magn. Reson.* **1982**, *49*, 341.
(14) Schmidt-Rohr, K.; Clauss, J.; Spiess, H. W. *Macromolecules* **1992**, *25*, 3273.
(15) Komoroski, R. A.; Mandelkern, L. *J. Polym. Sci., Polym. Symp.* **1976**, *54*, 201.
(16) Spiess, H. W. *Colloid Polym. Sci.* **1983**, *261*, 193.
(17) Opella, S. J.; Frey, M. H. *J. Am. Chem. Soc.* **1979**, *101*, 5854.
(18) Chung, G. C.; Kornfield, J. A.; Smith, S. A. *Macromolecules* **1994**, *27*, 964.
(19) Le Menestrel, C.; Kenwright, A.; Sergot, P.; Laupretre, F.; Monnerie, L. *Macromolecules* **1992**, *25*, 3020.
(20) VanderHart, D. L. *Macromol. Chem., Macromol. Symp.* **1990**, *38*, 125.
(21) McBrierty, V.; Douglass, D.; Kwei, T. *Macromolecules* **1978**, *11*, 1265.
(22) Clauss, J.; Schmidt-Rohr, K.; Spiess, H. W. *Acta Polym.* **1993**, *44*, 1.
(23) Li, S.; Rice, D. M.; Karasz, F. E. *Macromolecules* **1994**, *27*, 2211.
(24) White, J. L.; Mirau, P. A. *Macromolecules* **1994**, *27*, 1648.
(25) Kaplan, S. *Macromolecules* **1993**, *26*, 1060.
(26) Angerman, H.; ten Brinke, G.; Erukhimovich, I. *Macromolecules* **1996**, *29*, 3255.
(27) Fredickson, G.; Milner, S.; Leibler, L. *Macromolecules* **1992**, *25*, 6341.
(28) Pakula, T.; Matyjaszweski, M. *Makromol. Theory Simul.* **1996**, *5*, 987.

MA9716701